High Temperature Free Radical Polymerization. 1. Investigation of Continuous Styrene Polymerization

J. D. Campbell

Johnson Polymer, Innovatielaan 1, NL-8440 AJ, Heerenveen, The Netherlands

F. Teymour

Department of Chemical Engineering, Illinois Institute of Technology, Chicago, Illinois 60616

M. Morbidelli*

Swiss Federal Institute of Technology Zurich, Laboratorium für Techniche Chemie/LTC, ETH-Höggerberg/HCl, CH-8093 Zurich, Switzerland

Received April 25, 2002; Revised Manuscript Received March 27, 2003

ABSTRACT: An experimental study of the high-temperature polymerization of styrene in a CSTR, investigating the effect of reaction temperature (260−343 °C), and residence time (5−90 min) on monomer conversion and average molecular weight and distribution is reported. A kinetic analysis of these experimental data demonstrates that the dominant chain production reaction is backbiting followed by β-scission. In this reaction series, a chain end radical abstracts a hydrogen in a characteristic location down the chain, and subsequently undergoes β-scission, producing two smaller fragments, a radical and a terminally unsaturated polymer chain. It is found that the large variation of the average molecular weight observed in the considered range of operating conditions is strongly correlated to the ratio of the rate of propagation to that of backbiting/β-scission. Further kinetic analysis, based on the estimated activation energy of 77.5 kJ/mol for this reaction series, suggests that β-scission is the rate controlling step.

Introduction

High-temperature polymerization is a class of commercially important processes characterized by their high rates of productivity. Applications of these processes abound as attested to by a large body of patents.[1−5] The high polymerization temperatures involved in these processes (>180 °C and often >250 °C) lead to fast reaction kinetics, resulting in high monomer conversion (typically greater than 85%), at relatively short residence times. Under these reaction conditions, a linear, low molecular weight polymer is produced, often accompanied by high amounts of low molecular weight oligomeric species. Recent developments have led to high-temperature processes that produce high molecular weight hyperbranched polymer.[6,7] The continuous high-temperature polymerization of styrene between 250 and 350 °C is the subject of this study.

This polymerization process has been studied extensively due to its unique characteristics. In addition to those noted above, styrene is well-known to self-initiate at high temperatures to such an extent that chemical initiators are typically unnecessary. This thermal initiation mechanism has been the focus of the early studies in this field. A large effort was spent in determining and refining the complex mechanism of the initiation reaction.[8−13] In addition, it was observed that low molecular weight oligomers are formed during polymerization, and additional effort was spent to identify and determine their relationship to the thermal initiation mechanism.[14,15] In general, these studies were limited to temperatures less than 180 °C, below that of the present study.

The first attempts to understand the kinetics of this polymerization at temperatures above 180 °C were made by Hui and Hamielec.[16] They studied the bulk thermal polymerization of styrene in ampule reactors between 100 and 200 °C. They confirmed that the thermal initiation kinetics was third order in monomer, in agreement with the initiation mechanism first proposed by Mayo.[8] The kinetics of the system was successfully modeled, with the exception of the molecular weights for which using the classical termination controlled model was found to be unsatisfactory, and an empirical relationship had to be introduced. Hussain and Hamielec[17] extended this work to 230 °C and confirmed the initiation and monomer depletion kinetics.

Continuous high-temperature thermal polymerization of styrene in a CSTR was first reported by Hamielec et al.,[18] who studied experimentally the relationships between molecular weight and both temperature and reactor residence time. They found that the molecular weight was inversely proportional to the reaction temperature as well as the CSTR residence time. In this case, the model of Hui and Hamielec[16] was found unable to describe the molecular weights, and it was suggested that the cause for the poor model/experimental fit was degradation and unzipping of the polymer chains, reactions likely to occur at these extreme temperatures. Although they indicated some of the challenges to be met by predictive modeling when including scission and degradation reactions, this was not attempted. Hamielec et al.[18] also identified and measured oligomer concentrations, specifically triphenylhexene and cyclic trimers, showing that the amount of oligomers increases with increasing temperature and residence time. Kirchner et al.[19] also studied the polymerization of styrene in a

* To whom all correspondence should be addressed

10.1021/ma0206422 CCC: $25.00
Published on Web 06/24/2003

CSTR, although at lower temperatures than either the Hamielec work or that of the present study. In addition, Spychaj[20] studied the polymerization of styrene−acrylic acid copolymers in a CSTR at high temperatures in an attempt to identify the volatile oligomer production mechanisms.

In this work, we are revisiting this commercially important polymerization process, with the ultimate goal of providing a more detailed understanding of the mechanistic steps that govern its development. Specifically, we analyze the molecular weight data as a function of temperature and residence time to determine the relative contributions of the polymerization and degradation reactions on the molecular weight development and oligomer formation. As this experimental analysis helps determine the dominating mechanistic reaction steps, it enables the development of a mathematical model capable of fully describing the polymerization process. The second part[21] of this work presents the mathematical model to describe this system, and further analysis of the experimental results using advanced analytical methods is discussed elsewhere.[22]

Kinetic Mechanism

The mechanism for this polymerization is a complex combination of thermal initiation, polymerization and degradation reactions, all of which must be considered in our analysis. The reactions that are known to occur at the high temperatures of this study are presented in what follows and are shown in Figure 1, parts a−g.

Thermal Initiation. The thermal initiation mechanism first proposed by Mayo[8] was further refined by many researchers, culminating in the present, well-established understanding. Styrene monomer forms a Diels−Alder adduct, which can undergo molecule induced homolysis to produce two radicals, each capable of initiating polymerization, as shown in Figure 1a.

Degradation. The high temperature (>250 °C) of this polymerization extends into the range where degradation reactions become important. Polymer degradation occurs when polymer chains break into smaller fragments, thus reducing the molecular weight, and in some cases producing low molecular weight oligomers. The thermal degradation of polystyrene has been the subject of study for many years,[23−29] and the main reactions responsible for polymer chain degradation are well-known and understood.

In general, the first step in the degradation process is the production of a midchain radical, which is formed by abstraction of a hydrogen from a polymer chain, either through a chain transfer reaction or thermal abstraction. Once the midchain radical is formed, the chain can undergo β-scission, in which the carbon−carbon bond in the "β" position relative to the midchain radical breaks, forming two smaller fragments, one a radical and the other a terminally unsaturated polymer chain. The position of the hydrogen abstracted on the polymer chain determines the size of the fragments formed. Therefore, a random hydrogen abstraction such as chain transfer to polymer or thermal abstraction, results in the formation of random sized fragments, as shown in Figure 1b. In addition, it is known[25−28,30,31] that characteristic hydrogen abstraction, sometimes referred to as backbiting, can also occur. In this case, the chain end folds back onto the polymer chain and abstracts a hydrogen from a specific location down the chain, thus producing characteristic length radical and polymer fragments after β-scission occurs, as shown in Figure 1c. The third, fifth, and seventh carbons from the chain end are the most favored positions for abstraction,[30] although the fifth position is particularly favorable due to the formation of the conformationally favored six-membered ring transition state. The midchain radical formed by the 1:5 backbiting hydrogen abstraction can undergo β-scission in one of two possible "β" positions, to produce either (i) the characteristic trimer fragment, 2,4,6-triphenyl-1-hexene, or (ii) the characteristic dimer radical, shown in Figure 1c. Similarly, hydrogen abstraction from the third carbon from the chain end followed by β-scission produces the dimer oligomer, 2,4 diphenyl-1-butene, and abstraction from the seventh carbon produces the tetramer oligomer, 2,4,6,8-tetraphenyl-1-octene. The β-scission reaction can also occur on the chain end (depropagation), shown schematically in Figure 1c.

The polymer fragment produced by the β-scission reaction has a terminal unsaturation, capable of addition with a growing radical. This reaction, called addition−fragmentation, also produces a midchain radical that can undergo β-scission in either of the two "β " possible positions, as shown in Figure 1d.

Polymer chains exposed to extremely high temperatures can undergo spontaneous carbon−carbon bond fission,[23−25] shown in Figure 1e. In this reaction, the chain breaks randomly without being preceded by a hydrogen abstraction, producing two fragments, each with a radical on the chain end. This reaction has a very high activation energy[28,30] and would be expected to be negligible at all but the highest temperatures of this study.

Polymerization. In addition to propagation and termination of chain end radicals, it is possible that midchain radicals could also propagate with monomer, or terminate with another polymer radical, as shown in Figure 1, parts f and g, respectively. However, C^{13} NMR analysis of polymers, made under the conditions[22] of this study, has shown that the occurrence of propagation (head to tail) and termination (head to head) branching is below the NMR detection limit of 1 branch point per 110 monomer units and is therefore neglected in our analysis. Chain transfer to monomer has also been neglected in the following for two reasons. On one side, the hydrogens associated with the secondary benzylic carbons on the polymer chain are significantly more extractable than those on the monomer, as evidenced by ampule experimental data.[13] On the other, we are dealing with a continuous stirred tank reactor and since conversion is high, the concentration of monomer is a couple of orders of magnitude lower than that of backbone benzylic carbons.

Experimental Section

The nature of high temperature polymerization, which involves fast propagation kinetics, poses many challenges to the successful experimental investigation. Batch reactors or ampules are usually preferred for kinetic studies since they provide the potential to collect data at low monomer conversion. However, these reactors are characterized by a finite heating time, which in this case is of the same order as the reaction time. Therefore, it is impossible to ensure isothermal conditions in batch ampules since a significant amount of reaction occurs during the heat up period. CSTRs have the advantage that they can be operated isothermally and, due to typically low viscosity values, homogeneously and thus are best suited for high-temperature studies. However, experimental

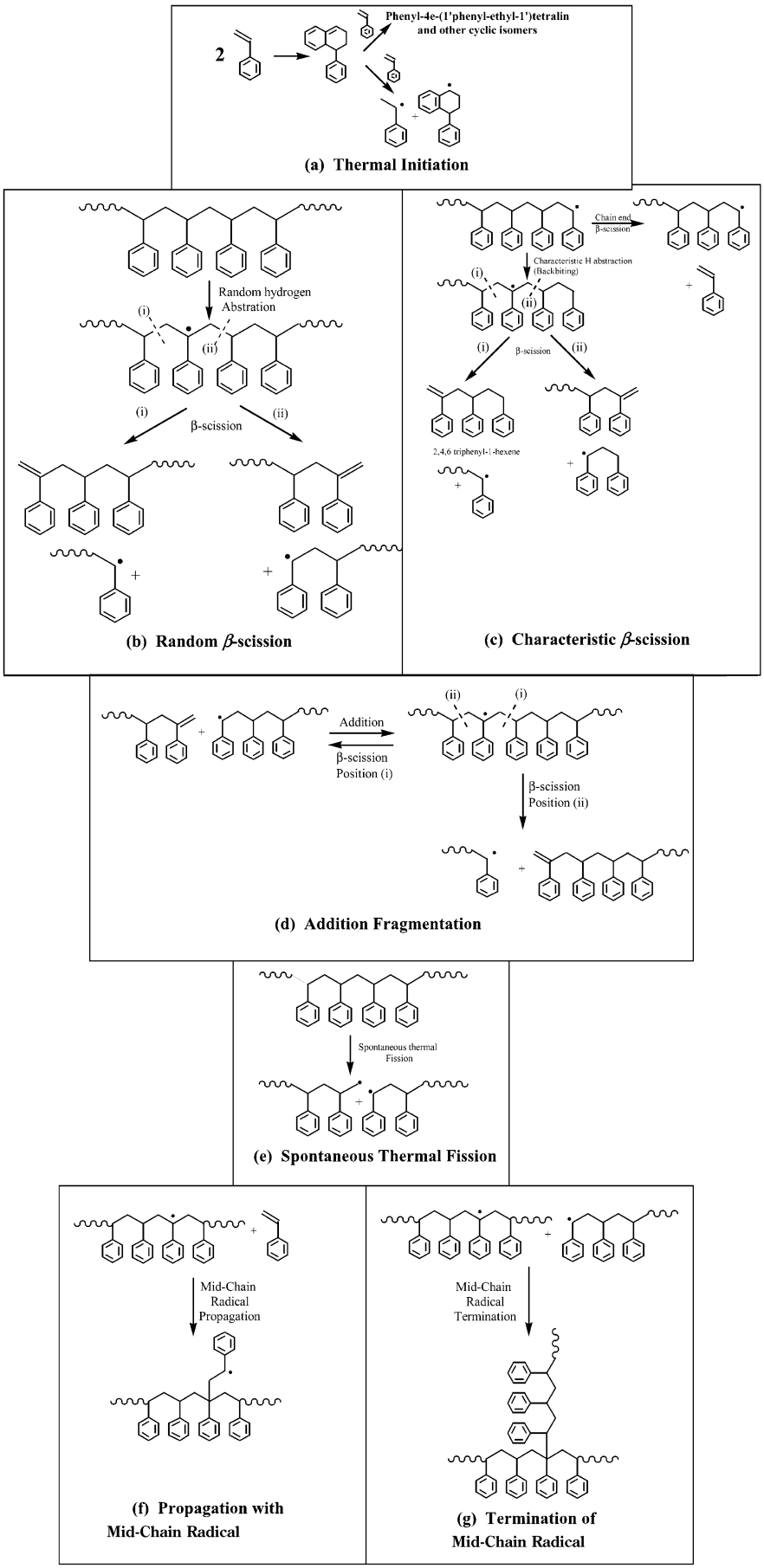

Figure 1. Reaction mechanisms: (a) thermal initiation, (b) random β-scission, (c) characteristic β-scission, (d) addition−fragmentation, (e) spontaneous thermal fission, (f) propagation with midchain radical, and (g) termination of midchain radical.

Table 1. Experimental CSTR Reaction Conditions, Temperature (T), Residence Time (RT), Monomer Conversion (X), the Relative Error from the CSTR Mass Balance (MB_{err}), and Number (M_n) and Weight-Average (M_w) Molecular Weights

T (°C)	RT (min)	X (%)	MB_{err}(%)	M_n	M_w
330	5	90.01	1.5	825	1260
316	5	89.54	3.1	1112	2706
288	5	79.00	4.7	2754	7042
260	5	69.00	0.6	5747	18 478
343	15	94.22	1.9	422	571
316	15	94.83	2.3	808	1548
288	15	93.66	5.1	1708	4047
260	15	87.44	2.9	3712	9567
343	30	95.84	3.2	367	453
316	30	97.18	2.4	615	1017
288	30	93.12	0.0	1280	2925
260	30	91.62	0.0	2656	5807
343	60	94.85	1.6	315	371
316	60	96.48	4.1	512	720
288	60	97.85	0.0	963	2042
260	60	95.42	1.5	1769	3993
343	90	95.44	3.0	309	351
316	90	96.99	3.1	464	641
288	90	96.85	2.9	750	1216
260	90	98.02	2.0	1400	4021
316[a]	15	84.56	3.5	682	1316
316[b]	15	92.38	3.1	782	1428

[a] Feed: 25% xylene/75% styrene. [b] Feed: 10% xylene/90% styrene.

limitations do exist with the CSTR, such as difficulty obtaining low conversion steady states due to the fast polymerization kinetics. The extremely low reactor residence times required to obtain such steady states are beyond what is physically possible due to a combination of heat transfer and mixing limitations. The high monomer feed rates associated with low residence times make isothermal operation unattainable, and adequate mixing of reactor contents difficult. For this reason, the minimum attainable residence time obtained was 5 min, and consequently all steady states obtained had relatively high monomer conversions.

The experimental protocol used in this study involved the high temperature thermal polymerization of styrene. Steady-state operation at 260, 288, 316, and 343 °C was achieved and polymer samples were collected. Five residence times (5, 15, 30, 60, and 90 min) were used at each temperature, resulting in a total of 20 experiments. In all cases, thermal initiation of styrene was the only radical source. Two additional experiments were performed to study the effect of solvent concentration on molecular weight. Table 1 summarizes the operating conditions of all the experiments performed together with the measured average molecular weights and monomer conversions. The amount of monomer fed over a specific time was known, and this was compared to the amount of distillate (unreacted monomer) plus polymer produced over the same period, to calculate the error in the overall mass balance. This is also presented in Table 1.

The polymers were produced using a 475 mL continuous stirred tank reactor, schematically shown in Figure 2. The reactor was equipped with an electric heating jacket, a magnetic drive agitator, and a single pitched blade turbine, operating at 2500 rpm to ensure good mixing. The feed was continuously fed to the reactor from a monomer feed tank via a positive displacement pump, to a subsurface location adjacent to the turbine agitator, thus ensuring a maximum level of shear and mixing. The flow rate of monomer was measured using a MicroMotion mass flow meter (approximate relative error of 1%), and controlled with a PID feedback controller. The reactor was operated liquid full and the product was removed continuously through an outlet at the top of the reactor. Reactor pressure was controlled at a constant 200 psia (for all experiments) by a pressure regulator valve, located on the exit stream. The temperature in the reactor was controlled by manipulation of the power output to the electric jacket. The

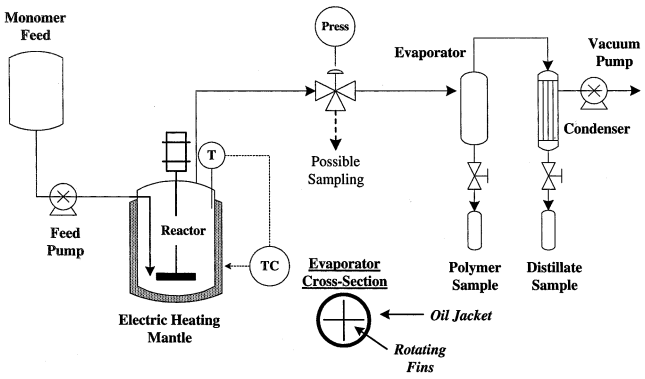

Figure 2. Schematic diagram of experimental apparatus.

reactor residence time was manipulated by varying the monomer feed rate. The reactor was operated for a time equal to five residence times prior to sampling to ensure steady-state operation.

The product was continuously fed from the reactor to a thin film evaporator that separated the polymer from the unreacted monomer and any byproducts formed. This equipment consisted of an oil-jacketed, cylindrical chamber that had four rotating, perpendicular blades. The blades rotate at a small distance from the wall, forming a thin film for optimal mass transfer of the volatile materials. Once the steady state was reached, the polymer produced over a 20-min interval was isolated in a closed sampling vessel that was immersed in an ice bath to quench any further reaction. The distillate (unreacted monomer and byproducts) was condensed and collected in a closed sample container. The residual monomer from the polymer and distillate samples were analyzed by gas chromatography and added together to calculate the total unreacted monomer. The evaporator and condenser were operated under vacuum to increase the efficiency of the evaporator. Further details about the experimental procedure are discussed elsewhere.[22]

Analytical Methods

The molecular weights of the polymers were determined by GPC, equipped with a refractive index detector. For all polymers with sufficiently low molecular weight (all those made above 260 °C), a GPC system, denoted GPC(1), particularly well suited to separate low molecular weight polymers and oligomers was used. This system was a Waters 2690 GPC, using a Shodex guard column (50 mm long, 6 mm ID) and a Shodex HF-2002 (exclusion limit: 5000, 200A Styragel packing) column. Eight narrow polystyrene standards between 104 and 10 000 Da were used to calibrate this system. This column set exhibited excellent low molecular weight resolution, making precise oligomeric determination possible. However, the relatively low exclusion limit of this column set made it impossible to measure the highest molecular weight samples in the study, typically those made at 260 °C. In these cases, the columns used were two Pl-gel mixed bed columns each with 10 μm particle size poly(styrene) beads, with a single Pl-gel preparative guard column (GPC(2)). A total of 15 narrow polystyrene standards between 104 and 3 000 000 Da were used to calibrate this system. Since this column set was applicable to a much broader range of molecular weights, resolution between the low molecular weight oligomers was lost when using this column set. The molecular weight averages were calculated according to Shortt,[32] and the molecular weight distributions were represented using the differential log MWD.

The evaporation system used to separate the unreacted monomer from the polymer also removed small amounts of low molecular weight oligomers. Since the characterization of the low molecular weight oligomers is crucial in this work, all the distillates collected from the evaporator were analyzed by GPC. The overall GPC distributions were calculated by the addition of the polymer and distillate GPCs, weighted by the appropriate ratio determined from the mass balance. Oligomer

concentrations were calculated by integration of the appropriate portion of the overall weight fraction distributions. The accuracy of this procedure, which relies on the use of a refractive index detector, in determining the oligomer concentrations has been verified by comparison to the results obtained by gravimetry of the corresponding fractions obtained by preparative GPC.[22]

Results and Discussion

Initiation and Monomer Consumption Kinetics. In this system, the thermal initiation of styrene is the only source of radicals. The effective rate of initiation is third order in monomer,[16] and therefore, in the absence of a dead polymer chain degradation, the rate of radical generation (R_I) is given by

$$R_I = 2k_I[M]^3 \tag{1}$$

At extreme temperatures, spontaneous polymer fission whereby a polymer chain has sufficient thermal energy to break into two smaller radical chains, can occur. However, this effect is considered negligible under the conditions of this study and is not included as a source of radicals in the present model. Therefore, assuming the quasi steady state on the radical concentration and neglecting radical outflow[22] from the CSTR, the concentration of radicals is given by

$$[R^\bullet] = \left(\frac{2k_I[M]^3}{k_{tc} + k_{td}}\right)^{1/2} \tag{2}$$

where

$[R^\bullet]$ = radical concentration (mol/L)

k_I = rate constant for thermal initiation ($L^2/mol^2/s$)

k_{tc} = rate constant for termination by combination (L/mol/s)

k_{td} = rate constant for termination by disproportionation (L/mol/s)

$k_{\beta SE}$ = rate constant for depropagation (1/s)

[M] = monomer concentration (mol/L)

The rate of propagation (R_p), given that polymer chains can depropagate at these high temperatures is given as

$$R_p = (k_p[M] - k_{\beta SE})[R^\bullet] \tag{3}$$

Substitution of eq 2 into eq 3 gives the overall rate of polymerization. This rate depends solely on the monomer concentration and the reactor temperature, as shown by

$$R_p = \left(\frac{2k_I}{k_{tc} + k_{td}}\right)^{1/2} (k_p[M] - k_{\beta SE})[M]^{3/2} \tag{4}$$

The monomer is consumed by propagation and thermal initiation, and produced by depropagation of growing polymer radicals, which can occur under the temperature conditions of this study. The monomer concentration (and consequently the monomer conversion) can be obtained by the solution of the differential monomer balance for a CSTR, shown below:

$$\frac{d[M]}{dt} = \frac{[M]_f - [M]}{\theta} - \left(\frac{2k_I}{k_{tc} + k_{td}}\right)^{1/2} (k_p[M] - k_{\beta SE})[M]^{3/2} - k_I[M]^3 \tag{5}$$

where

$[M]_f$ = monomer feed concentration (mol/L)

θ = reactor residence time (s)

Substituting eqs 4 and 2 into eq 5, and setting the accumulation term to zero, gives the steady-state monomer concentration as the solution of the following equation:

$$0 = [M]_f - [M] - \theta\left[(k_p[M] - k_{\beta SE})\left(\frac{2k_I[M]^3}{k_{tc} + k_{td}}\right)^{1/2} + k_I[M]^3\right] \tag{6}$$

This model was used to estimate the frequency factors for the thermal initiation and the chain end β-scission (depropagation) rate constants directly, by fitting the experimental monomer conversions at the various temperatures and residence times investigated, using unweighted least-squares fitting. Literature values of the activation energies for chain end β-scission[29] and thermal initiation[16] rate constants were used. Values for frequency factors and activation energies for the propagation[33] and the termination rate constants[34] obtained from pulsed laser experimentation were used. Pulsed laser experimentation for the determination of the propagation and termination rate constants is performed at significantly lower temperatures than this study, making extrapolation to higher temperatures questionable. However, since these values agree well with those reported from previous high temperatures[16] studies of poly(styrene), we have used the most widely accepted pulsed laser results. The values of all parameters are summarized in Table 2. The estimated values of the frequency factors compared reasonably with literature values, also shown in Table 2. The obtained model/experimental comparison of the monomer conversion as a function of temperature and residence time is shown in Figure 3, indicating an adequate fit of the data. The relative error between the model and experimental values is generally less than 2%, with the exception of a 14% relative error for the data point at 260 °C and 5 min residence time.

Molecular Weight Distributions. The high-temperature polymerization of styrene is characterized by

Table 2. Estimated Kinetic Parameters for Monomer Consumption as Given by Eq 6

parameter	reaction	A_0 (L/mol/s or $L^2/mol^2/s$ or 1/sec)	E_A/R (K)	reference	
				A_0	E_A/R
k_p	propagation	4.3×10^7	3910	33	33
k_I	thermal initiation	6.3×10^5 [b]	13 810	*a*	16
k_{tc}	termination by (combination)	1.06×10^9	753	34	34
k_{td}	termination (disproportionation)	1.52×10^8	753	34	34
$k_{\beta SE}$	chain end β-scission	8.3×10^{11} [c]	10 600	*a*	29

[a] Estimated from the present study. [b] Hui et al.[16] estimated 2.2×10^5 ($L^2/mol^2/s$). [c] Kruse et al.[29] estimated 2.6×10^{12} (1/s).

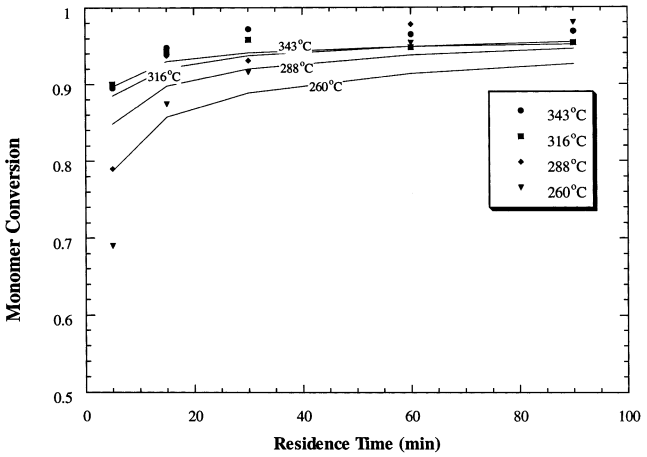

Figure 3. Monomer conversion as a function of residence time for various temperature values. The curved lines indicate the results given by eq 6.

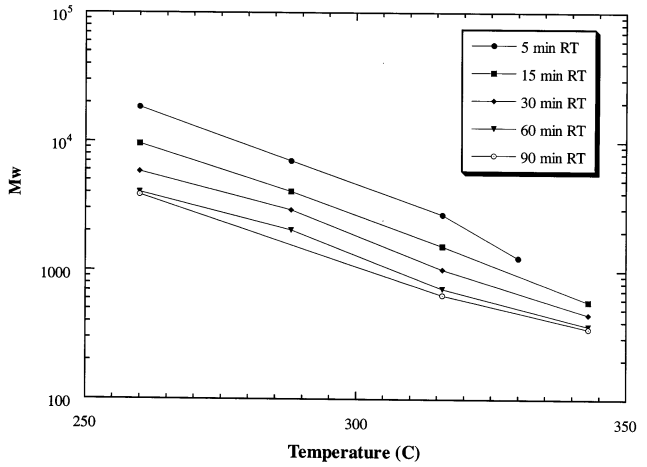

Figure 4. Experimental weight-average molecular weight M_w as a function of temperature for various values of the residence time.

the production of low average molecular weight polymer, and varying levels of low molecular weight oligomers. The GPC column set used was specifically chosen to resolve these oligomers. In the following, we discuss the average molecular weight behavior as well as the molecular weight distributions.

Figure 4 shows the experimental weight-average molecular weight as a function of temperature at various residence times (RT). The molecular weight decreases with increasing temperature, and with increasing RT. The molecular weight distributions (MWD) provide additional clues to the nature of the dominant mechanisms in this polymerization process. Parts a−e of Figure 5 show the effect of temperature on the MWDs at various residence times, and Figure 6 shows one example of the effect of residence time at various reaction temperatures. The multiple peaks exhibited by the MWD represent the significant population of low molecular weight oligomers, which are at least partially resolved by the GPC. It can be seen that the concentration of these oligomers increases with both temperature and residence time, although there is no shift in their molecular weight.[36] The fact that the molecular weight of the oligomers does not shift, despite the wide range of temperatures and residence times investigated, indicates the presence of a characteristic scission reaction occurring at the same place on the chain, producing oligomers of the same length regardless of reaction conditions. Intramolecular hydrogen abstraction, or backbiting, followed by β-scission is known[14,27,28] to occur in the thermal degradation of polystyrene, and is the likely explanation for these observations. The chain end radical can abstract a variety of hydrogens down the chain, however the most likely are the benzylic hydrogens on the third, fifth and seventh tertiary carbons from the chain end. The activation energy required to abstract hydrogen from the secondary methylene carbons is approximately twice as high[30] and not as likely. The 1:5 transfer is the most favorable abstraction due to the entropically favored six-member ring that is formed, as shown in Figure 1c. The transition state for the 1:3 backbiting reaction is more highly strained and therefore less favorable than the 1:5 abstraction. Oligomers seen in Figures 5 and 6 have been positively identified[22] as the unsaturated dimer (2,4-diphenyl-1-butene: M_w = 208 Da) and trimer (2,4,6-triphenyl-1-hexene: M_w = 312 Da), the products of the 1:3 and 1:5 backbiting reactions. The structure of the 1:7 backbiting product (2,4,6,8-tetraphenyl-1-octene) was instead inferred from the location of the corresponding GPC peak with respect to that of the other two oligomers, which implies a molecular weight of approximately 416 Da.[22] The dominance of these three oligomers in the distributions indicates the significant nature of the backbiting and β-scission reactions in determining the molecular weight.

Development of the Kinetic Mechanism. The formulation of a kinetic mechanism for this polymerization system must be consistent with the molecular weight development shown in Figures 4−6. Although it is clear that backbiting and β-scission reactions are important in producing the characteristic oligomers that dominate the molecular weight distribution, it is not immediately clear whether this reaction dominates also the molecular weight development of the polymer chains. Typically, bimolecular termination is the dominant reaction for production of "dead" polymer chains, but chain transfer reactions besides backbiting, such as chain transfer to polymer followed by β-scission, could play an important role. In addition, chain transfer to small molecules such as the Diels−Alder adduct, postulated by various authors[13,16,17,35] to control the molecular weight, could also have an impact. Distinction between chain transfer and bimolecular termination control is the first step in understanding the MWD in this polymerization and can be achieved by the following kinetic analysis. In particular, we consider in the following only the backbiting/β-scission reaction and will come back later to the other chain transfer reactions.

In the case where bimolecular termination controls the molecular weight, the molecular weight (or number-average degree of polymerization D_n) is proportional to the ratio between the rate of propagation and the rate of termination as shown by

$$D_n \propto \frac{k_p[M]}{(k_{tc} + k_{td})[R^\bullet]} \tag{7}$$

Substituting the expression for [R•] from eq 2 yields

$$D_n \propto \frac{k_p}{\{2k_I(k_{tc} + k_{td})\}^{1/2}[M]^{1/2}} \tag{8}$$

Since $M_n = D_n M_m$, where M_m is the monomer molecular weight, and the activation energies for termination and

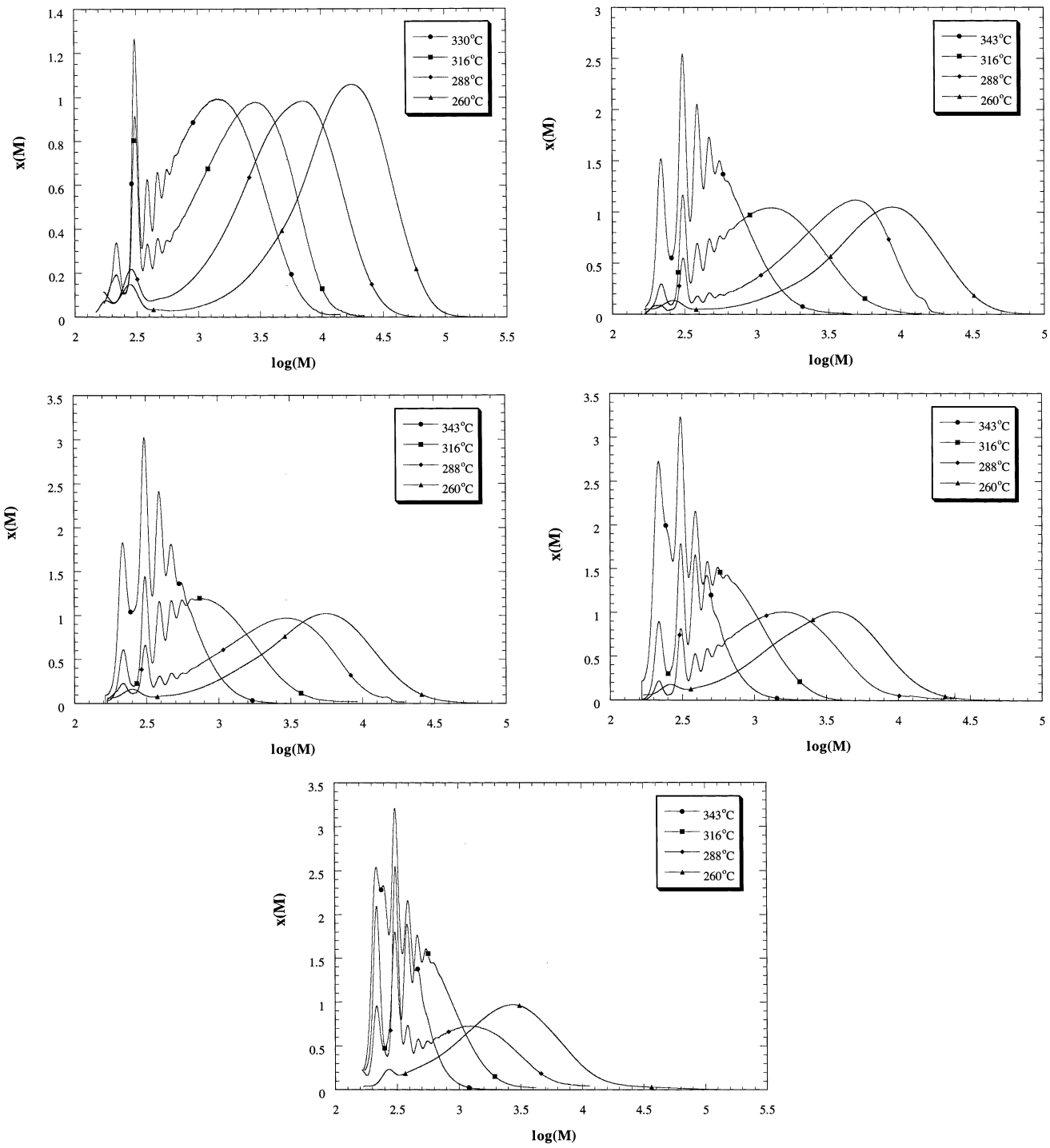

Figure 5. Molecular weight distributions for various temperature values at (a) 5, (b) 15, (c) 30, (d) 60, and (e) 90 min residence time.

disproportionation are equal, plotting $\ln(M_m[M]^{1/2})$ vs $1/T$ should yield a straight line if the molecular weight is controlled by bimolecular termination reactions. This relationship is valid for systems that exhibit a negligible gel effect, which is the case in this system due to the extremely low viscosities encountered under the experimental conditions of this study.

The case where backbiting/β-scission is the dominant chain termination mechanism presents a different kinetic situation, since this reaction is first order with respect to the radical concentration. Thus, indicating the rate of chain production by backbiting/β-scission by $k'_B[R^\bullet]$, we get

$$D_n \propto \frac{k_p[M][R^\bullet]}{k'_B[R^\bullet]} \propto \frac{k_p[M]}{k'_B} \tag{9}$$

where k'_B is a lumped kinetic parameter whose nature we discuss later in more detail. From eq 9, it is seen that in this case, the molecular weight is only a function of temperature and monomer concentration, and not of the concentration of radicals. Therefore, plotting $\ln(M_n/[M])$ vs $1/T$ should yield a straight line if backbiting is the molecular weight controlling reaction.

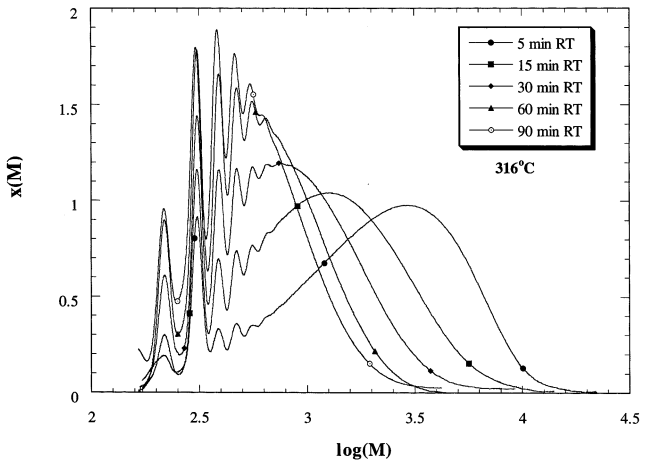

Figure 6. Molecular weight distributions for various residence time values at 316 °C.

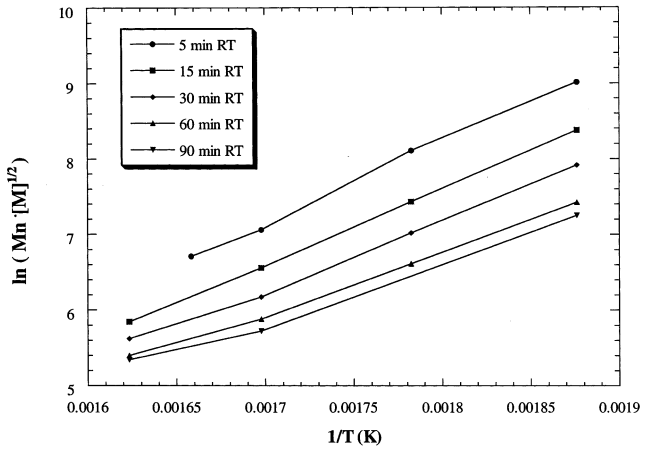

Figure 7. Linearization for termination controlled kinetics: $\ln(M_n[M]^{1/2})$ vs $1/T$.

The different functional dependency of the molecular weight depending on whether bimolecular termination or backbiting/β-scission controls, as given by Equations 8 and 9, respectively, provide a kinetic method to differentiate between these two regimes. This kinetic analysis depends on the monomer concentration, and it must be noted that large errors inherently result in the experimental determination of the monomer concentration ([M]) at the high conversions encountered. In this low [M] regime, constant absolute error in measurement of the monomer concentration result in large relative errors. Therefore, to minimize the effect of measurement error on the analysis of the molecular weight data, monomer concentrations calculated using the model were used in the following kinetic analysis. Since these are based on published kinetics with a high degree of confidence, which we have seen to well reproduce also our own monomer conversion data, it is deemed that there is less error in the model calculation of the monomer concentration than in its experimental determination.

Figure 7 shows the $\ln(M_n[M]^{1/2})$ vs $1/T$ plot, representing the case of bimolecular termination control. It is clear from this plot that the $[M]^{1/2}$ dependence is not able to capture the variation in the residence time, which leads to points lying on different straight lines. This indicates that bimolecular termination is not the dominant mechanism for molecular weight development. In contrast, it is seen from Figure 8, when plotting

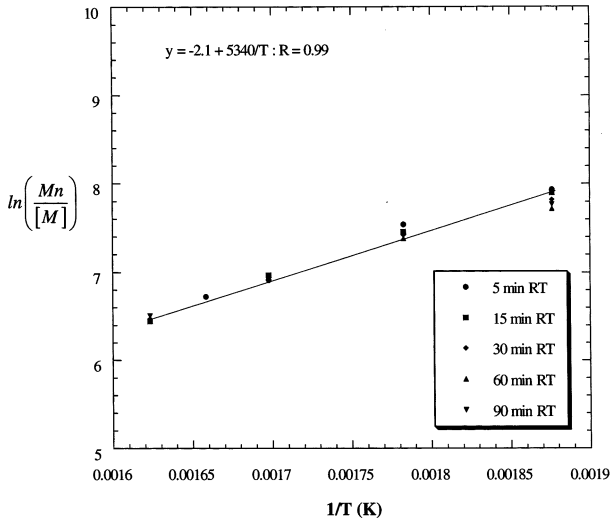

Figure 8. Linearization for chain transfer controlled kinetics: $\ln(M_n/[M])$ vs $1/T$.

$\ln(M_n/[M])$ vs $1/T$, that the residence time effect is removed and the measured molecular weights collapse onto a single line, at least within the approximations implicit in an oversimplified analysis of this type. This suggests that the molecular weight is not controlled by bimolecular termination, and it is instead consistent with backbiting followed by β-scission. On the other hand, there are other chain transfer reactions that, like backbiting, exhibit a first-order dependence with respect to the radical concentration and therefore would lead to expressions of the average molecular weight similar to eq 9. In the next section, we will deepen the analysis in order to discriminate among various chain transfer mechanisms.

The Dominating Chain Transfer Mechanism. Further kinetic analysis can assist in determining which chain transfer reaction is dominant. As a first step we further analyze the backbiting/β-scission reaction, which is actually constituted by two series reactions, i.e., backbiting and β-scission, and investigate which is the rate-determining step, thus providing physical insight on the nature of the lumped kinetic parameter k'_B introduced in eq 9. From the slopes of the straight lines in Figure 8 and eq 9, we can estimate, knowing the activation energy for propagation, the activation energy of the lumped backbiting/β-scission rate constant, k'_B. In particular, a value of 77.5 kJ/mol is obtained from the M_n data. This is similar in magnitude to β-scission reactions reported for the degradation of polystyrene,[29] and much larger than those typical for hydrogen abstraction in polystyrene.[29] This suggests that the rate-determining step in the chain termination process is the β-scission reaction, as it is demonstrated in the following analysis.

The midchain radical formed by backbiting can either remain in resonance until the β-scission occurs, or transfer to another site along the chain, or reversibly transfer back to the chain end. Although the reversible transfer is expected to prevail due to the proximity and favored configuration of the chain end with respect to the midchain, let us analyze each one of these two situations (i.e., with and without reversible transfer) in more detail. The first situation, where backbiting is assumed irreversible, can be described by the following

reaction scheme:

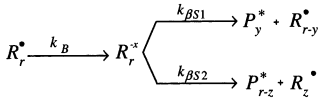

(10)

where

k_B = overall rate constant for the 1:3, 1:5, and 1:7 backbiting reactions

$k_{\beta S1}$ = rate constant β-scission in the first "β" position adjacent to the radical

$k_{\beta S2}$ = rate constant β-scission in the second "β" position adjacent to the radical

R_r^{-x} = midchain radical with "r" monomer units, and the radical located on the xth carbon from the chain end

P_r = polymer chain with length "r"

R_z^* = oligomeric radicals with length "z" , where $z = 1$, 2, or 3, formed by the 1:3, 1:5, and 1:7 backbiting reaction, respectively

P_y^* = oligomeric polymers with length "y" , where $y = 2$, 3, or 4, formed by the 1:3, 1:5, and 1:7 backbiting reaction, respectively

The total rate of production of polymer chains, including oligomers, is given by

$$\frac{dP}{dt} = (k_{\beta S1} + k_{\beta S2})\sum_{r=1}^{\infty}[R_r^{-x}] = k_{\beta S}\sum_{r=1}^{\infty}[R_r^{-x}] \quad (11)$$

Performing a balance on the concentration of midchain radicals R_r^{-x} gives

$$\frac{[R_r^{-x}]}{dt} = k_B[R_r^{\bullet}] - k_{\beta S}[R_r^{-x}] \quad (12)$$

Assuming the quasi-steady-state approximation (QSSA) for midchain radicals, the total rate of chain production is given by

$$\frac{dP}{dt} = k_B[R^{\bullet}] \quad (13)$$

which, by comparison with eq 9 indicates that, in this case, the lumped rate constant k'_B is actually equal to the backbiting rate constant, that is

$$k'_B = k_B \quad (14)$$

This mechanism implies that the midchain radicals accumulate until the rate of β-scission equals that of backbiting, and therefore the overall rate constant reflects hydrogen abstraction, not β-scission. As discussed above, the data in Figure 8 leads to an activation energy for k'_B of 77.5 kJ/mol, which is too large to be attributed to k_B, an hydrogen abstraction rate constant, thus leading to the conclusion that the reaction mechanism (10) is not feasible.

On the other hand, if reversible backbiting is assumed, the following reaction scheme can be considered:

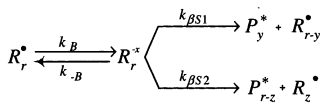

(15)

where

k_{-B} = Overall rate constant for the reverse 1:3, 1:5 and 1:7 backbiting reactions

As in the previous case, the rate of production of polymer, including oligomers, is given by

$$\frac{dP}{dt} = (k_{\beta S1} + k_{\beta S2})\sum_{r=1}^{\infty}[R_r^{-x}] = k_{\beta S}\sum_{r=1}^{\infty}[R_r^{-x}] \quad (16)$$

Applying the QSSA to the concentration of midchain radicals and substituting into eq 16 gives the total rate of chain production:

$$\frac{dP}{dt} = \frac{k_{\beta S}k_B}{k_{\beta S} + k_{-B}}[R^{\bullet}] \quad (17)$$

In the situation where β-scission is rate determining, the reverse backbiting reaction is much faster than β-scission ($k_{\beta S} \ll k_{-B}$), and then the following relation is obtained by comparison with eq 9:

$$k'_B = \frac{k_{\beta S}k_B}{k_{-B}} \quad (18)$$

Therefore, in the case of reversible backbiting, the lumped rate constant is a function of the β-scission rate. In addition, knowledge of the activation energies of the forward and backward reactions allow the calculation of the β-scission activation energy, which can then be compared to literature values for consistency. The activation energies for the forward and backward backbiting reactions have been calculated to be $E_{A(k_B)} = 52$ kJ/mol and $E_{A(k_{-B})} = 65$ kJ/mol, using the Evans–Polanyi parameters for the degradation of polystyrene as given by Kruse et al.[29] Since from the data in Figure 8 the value $E_{A(k'_B)} = 77.5$ kJ/mol has been estimated, from eq 18 we get $E_{A(k\beta_S)} = 90.5$ kJ/mol. This compares favorably with the value of 105 kJ/mol reported in the literature.[29] The consistency of this kinetic mechanism with the activation energy estimated from the molecular weight data allows us to imply that backbiting is reversible and β-scission is the rate controlling step.

Let us now consider the contribution of chain transfer to polymer (CTP) to chain production. Since we have found that the backbiting hydrogen abstraction is important, it is clear that we could expect the CTP reaction to be also important. However, it is unlikely that the midchain radical formed by CTP could be in equilibrium with the original radical since the two chains involved rapidly diffuse away from each other. Accordingly, we can have only a reaction mechanism similar to that described in the case of irreversible backbiting by eq 10. Since the rate of chain transfer to polymer is proportional to the concentration of polymer (Q_1), the molecular weight dependence in the case of

chain production dominated by CTP is given by

$$D_n \propto \frac{k_p[M]}{k_{fp}Q_1} = \frac{k_p[M]}{k_{fp}([M]_f - [M])} \tag{19}$$

or

$$D_n\left(\frac{[M]_f}{[M]} - 1\right) \propto \frac{k_p}{k_{fp}} \tag{20}$$

By comparison with eq 9, this relation implies that, according to the molecular weight data in Figure, the rate constant for chain transfer to polymer, k_{fp}, should have an activation energy value of the order of 77.5 kJ/mols, which is too large for a hydrogen abstraction reaction. Thus, we conclude that chain transfer to polymer cannot be the dominant chain production mechanism. A similar conclusion can be reached for the chain transfer to small molecules reaction, which in addition should also exhibit a dependence on the chain transfer agent concentration, which could vary significantly at the high temperatures involved.

One reaction that we have not mentioned so far is the addition−fragmentation reaction shown in Figure 1d, which is also a chain transfer reaction that could play a role in the molecular weight development. The kinetic scheme for this reaction is given by

$$R_{r-1,a} + P_{s,b}|_{b>1} \underset{k_{\beta S1}}{\overset{k_{AF}}{\rightleftharpoons}} R^{\oplus}_{r+s-1,a+b-1} \xrightarrow{k_{\beta S2}} R_{s+1,b-1} + P_{r,a+1} \tag{21}$$

where "*a*" and "*b*" represent the number of terminal double bonds on the radical and polymer chains, respectively, and $R^{\oplus}$ indicates a midchain radical. However, from the stoichiometry of this reaction we see that it does not contribute to monomer consumption nor does it affect the number of polymer chains, so that it clearly cannot have any effect on the average molecular weight, D_n.

The kinetic analysis presented above allows for a clear understanding of the complex temperature and residence time effects on the average molecular weight observed in Figure 4. As described by eq 9, the molecular weight is controlled primarily by the ratio of the rate of propagation to the rate of backbiting/β-scission, which is controlled by the β-scission step. This simple relationship predicts that the molecular weight is only a function of temperature and monomer concentration. When the temperature is increased, there are two effects on the molecular weight. First, since the activation energy of the β-scission reaction is significantly higher than that of propagation, the average molecular weight decreases at higher temperatures. Second, the absolute rate of propagation increases for increasing temperatures, thus lowering the monomer concentration and therefore further decreasing the molecular weight. The residence time on the other hand affects the average molecular weight in eq 9 only by impacting the monomer concentration. Longer residence times lead to lower monomer concentrations, resulting in lower molecular weight.

Solvent Effect. From the analysis above, it follows that any process change that affects the ratio of propagation to backbiting reaction rate should also affect the molecular weight and the concentration of oligomers. It is possible to change this reaction rate ratio, independently of previously studied residence time and temperature, by manipulating the solvent level. In particular, the addition of solvent to the reaction mixture reduces the monomer concentration, without varying either the temperature or the residence time, thus allowing for an independent experimental validation of the conclusion of the above kinetic analysis.

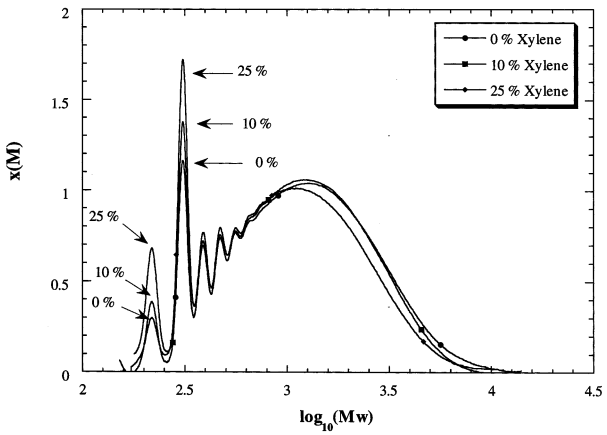

Figure 9. Weight fraction distribution at 316 °C and 15 min residence time for various solvent levels in the feed stream.

Figure 9 shows the effect on the molecular weight distribution of the solvent concentration in the feed mixture (i.e., *p*-xylene of 0, 10%, and 25%) to the polymerization feed mixture at 316 °C. It is seen that the overall molecular weight is reduced when solvent is added, as clearly evidenced by the reduction in the high molecular weight tail of the distribution. In addition, there is a significant increase in the concentration of all oligomers formed at higher levels of solvent. Although chain transfer to solvent could potentially explain the molecular weight behavior, it cannot account for the increase in the concentration of oligomers observed. Therefore, the combination of these two observations is in good agreement with the conclusion of our kinetic analysis as given by eqs 9 and 22. When the concentration of solvent increases, the rate of propagation relative to backbiting decreases. Therefore, the probability of a growing radical backbiting instead of propagating increases, consequently reducing the molecular weight while increasing the concentration of oligomers.

Conclusions

In this work, we have performed an experimental study of the thermal polymerization of styrene in a CSTR at temperatures between 260 and 345 °C and various residence times. The analysis of the obtained data allowed us to conclude that under these reaction conditions, backbiting followed by β-scission not only occurs to a significant extent, but its rate with respect to that of propagation, controls the average molecular weight development and oligomer formation. This conclusion is supported by a number of observations, including the following: (i) at any particular temperature, the molecular weight is only a function of monomer concentration and increases linearly with it, (ii) the activation energy of the molecular weight controlling reaction is similar to that of a β-scission reaction in polystyrene, (iii) the concentration of the oligomers, characteristic of the 1:3, 1:5, and 1:7 backbiting/β-scission reaction, depends on temperature and residence time in the same way as the average molecular weight does, and (iv) the addition of solvent reduces the

molecular weight and increases the concentration of the oligomers.

Thus, summarizing, the length of the polymer chains formed under these conditions is determined by how long the chain is able to propagate before it terminates through backbiting/β-scission. Since backbiting is a unimolecular reaction whose rate is not affected by the concentration of monomer, the concentration of monomer is the crucial variable in determining the chain length. Accordingly, reaction conditions that affect the concentration of monomer affect also the molecular weight and the amount of oligomers formed.

In the second paper in this series, these conclusions about the reaction mechanism are used to develop a mathematical model that simulates the kinetic behavior of thermal polymerization as well as the characteristics of the produced polymer chains in terms of length and end groups.

Acknowledgment. The authors would like to thank John Robertson of Johnson Polymer for performing the CSTR experimentation, and Johnson Polymer for supporting this work.

Notation

D_n = number-average degree of polymerization
E = activation energy
k_B = backbiting rate constant
k'_B = backbiting/β-scission lumped rate constant
$k_{\beta SE}$ = chain end β-scission rate constant (depropagation)
$k_{\beta S}$ = overall β-scission rate constant, $k_{\beta S1} + k_{\beta S2}$
$k_{\beta S1}$ = β-scission rate constant where the chain breaks in the first position with the β-position adjacent to the radical
$k_{\beta S2}$ = β-scission rate constant where the chain breaks in the second position with the β-position adjacent to the radical
k_{fp} = chain transfer to polymer rate constant
k_I = thermal initiation rate constant
k_p = propagation rate constant
k_{tc}, k_{td} = termination rate constant by combination or disproportionation
[M] = monomer concentration
$[M]_f$ = monomer concentration in the feed
M_m = monomer molecular weight
M_n = number-average molecular weight
M_w = weight-average molecular weight
$P_{r,a}$ = dead polymer chain of length r with a terminal double bonds
Q_i = overall ith moment of the polymer distribution
$[R^\bullet]$ = concentration of radicals
R_I = rate of thermal initiation
R_p = rate of monomer propagation
$R_{r,a}$ = radical chain of length r with a terminal double bonds
$R^{\oplus}_{r,a}$ = midchain radical of length r with a terminal double bonds
T = temperature
$x(M)$ = differential log weight fraction distribution
θ = reactor residence time

References and Notes

(1) Hamielec, A. E.; Lawless, G. P.; Schultz, H. H. US Patent 4,414,370, 1983.
(2) Schmidt, R. E.; Schultz, H. H.; Wilson, D. M. US Patent 4,-529,787, 1985.
(3) Brand, J. A.; Morgen, L. W. US Patent 4,546,160, 1985.
(4) Brandstetter, F.; Gausepohl, H.; Thiele, R. DE Patent 4,236,-058 A1, 1994.
(5) Hambrecht, J.; Volker, M.; Bankowsky, H.-H.; Wistuba, E. EPO Patent 0100444 B2, 1993.
(6)) Campbell, J. D.; Teymour, F. US Patent 5,986,020, 1999.
(7) Campbell, J. D.; Teymour, F. US Patent 6,265,511, 2001.
(8) Mayo, F. R. *J. Am. Chem. Soc.* **1968**, *90*, 1289.
(9) Brown, W. G.; Buchholz, K.; Kirchner, K. *Makromolekul. Chem.* **1969**, *128*, 130.
(10) Kirchner, V. K.; Buchholz, K. *Angew. Makromol. Chem.* **1970**, *13*, 127.
(11) Buchholz, K.; Kirchner, K. *Makromol. Chem.* **1976**, *177*, 935.
(12) Kauffmann, H. F.; Olaj, O. F.; Breitenbach, J. W. *Makromol. Chem.* **1976**, *177*, 939.
(13) Olaj, O. F.; Kauffmann, H. F.; Breitenbach, J. W. *Makromol. Chem.* **1977**, *178*, 2707.
(14) Kurze, V. J.; Stein, D. J.; Simak, P.; Kaiser, K. *Angew. Makromol. Chem.* **1970**, *12*, 25.
(15) Kirchner, K.; Riederle, K. *Angew. Makromol. Chem.* **1983**, *111*, 1.
(16) Hui, A.; Hamielec, A. E. *J. Appl. Polym. Sci.* **1972**, *16*, 749.
(17) Hussain, A.; Hamielec, A. E. *J. Appl. Polym. Sci.* **1978**, *22*, 1207.
(18) Hamielec, A. E.; MacGregor, J. F.; Webb, S.; Spychaj, T. In *Polymer Reaction Engineering*; Reichert, K. H., Geisler, W., Eds.; Hüthig and Wepf: New York, 1986; p 185.
(19) Kirchner, K.; Katzenmayer, T. In *Polymer Reaction Engineering*, Reichert, K. H., Geisler, W., Eds.; Hüthig and Wepf: New York, 1986; p 287.
(20) Spychaj, T.; Hamielec, A. E. *J. Appl. Polym. Sci.* **1991**, *42*, 2111.
(21) Campbell, J. D.; Morbidelli, M.; Teymour, F. *Macromolecules* **2003**, *36*, 5502.
(22) Campbell, J. D. Ph.D. Thesis, Swiss Federal Institute of Technology, Zurich, Switzerland, 2003.
(23) Jellinek, H. H. G. *J. Polym. Sci.* **1948**, *3*, 850.
(24) Jellinek, H. H. G. *J. Polym. Sci.* **1948**, *4*, 13.
(25) Madorski, S. L. *Thermal Degradation of Organic Polymers.* Polymer Reviews 7; Wiley: New York, 1964.
(26) Cameron, G. G.; MacCallum, J. R. *Rev. Macromol. Chem.* **1967**, *2*, 327.
(27) Schroder, U. K. O.; Ebert, K. H.; Hamielec, A. E. *Makromol. Chem.* **1984**, *185*, 991.
(28) Ebert, K. H.; Ederer, H. J.; Schroder, U. K. O.; Hamielec, A. E. *Makromolekul. Chem.* **1982**, *183*, 1207.
(29) Kruse, T. M.; Woo, O. S.; Broadbelt, L. J. *Chem. Eng. Sci.* **2001**, *56*, 971.
(30) Woo, O. S.; Broadbelt, L. J. *Catal. Today* **1998**, *40*, 121.
(31) Daoust, D.; Bormann, S.; Legras, R.; Mercier, J. P. *Polym. Eng. Sci.* **1981**, *21*, 721.
(32) Shortt, D. W. *J. Liq. Chromatogr.* **1993**, *16*, 3371.
(33) Buback, M.; Gilbert, R. G.; Hutchinson, R. Kumperman, B.; Kuchta, F. D.; Manders, B. B.; O'Driscoll, K. F.; Russel, G. T.; Schweer, *J. Macromol. Chem. Phys.* **1995**, *196*, 3267.
(34) Buback, M.; Kuchta, F. *Macromol. Chem. Phys.* **1997**, *198*, 1455.
(35) Olaj, O. F.; Kauffmann, H. F.; Breitenbach, J. W. *Polym. Lett. Ed.* **1977**, *15*, 229−233.
(36) The MWDs for polymers produced at 260 °C were measured using the GPC(2) column set, and as such the resolution of individual oligomers cannot be observed.

MA0206422